

# Marine Technology Society

Dynamic Positioning Conference

21 - 22 October, 1997

## Session 9

### Control Systems

---

#### High Performance Thrust Allocation Scheme in Positioning of Ships Based on Power and Torque Control

By: Asgeir J. Sørensen

*ABB (Oslo, Norway)*

Alf Kare Ådnanes

*ABB (Oslo, Norway)*

---

### Session Planners

Rec Stanbery: *Sedco-Forex Houston*

Don Weisinger *BP (Houston)*

# High Performance Thrust Allocation Scheme in Positioning of Ships Based on Power and Torque Control

Presented at Dynamic Positioning Conference, Houston, Texas

October 21-22, 1997

by

**Asgeir J. Sørensen and Alf Kåre Ådnanes**

ABB Industri AS  
P.O. Box 6540 Rodeløkka  
N-0501 Oslo, Norway  
Phone: +47 22 87 20 00  
Fax: +47 22 35 36 80

E-mail: asgeir.sorensen@noina.abb.no, alf-kare.adnanes@noina.abb.no

## ABSTRACT

Thruster and propeller devices may be of the type controllable pitch propeller (CPP) with fixed speed, controllable speed with fixed pitch propeller (FPP), or controllable pitch and speed in combination. In conventional positioning systems the final thruster pitch or speed set-point signals are determined from stationary propeller-force-to-speed/pitch relations based on data from the propeller manufacturer. However, these relations are strongly influenced by the local water flow around the propeller blades subject to hull design, operational philosophy, vessel motion, waves and water current. In this paper a method based on torque control and power control of the propeller and thruster devices is presented. Instead of calculating the propeller speed and pitch set-point signals based on stationary functions, the propeller-force-to-moment and -power relations are used. Power and torque control in combination gives a significant improvement in the performance and the stability of the electrical power plant network, while the positioning accuracy and bandwidth are improved as well.

## INTRODUCTION

Positioning systems such as dynamic positioning (Dynpos) systems, thruster assisted position mooring (Posmoor) systems, and autosail systems for marine, oil, and gas vessels have been subject to an increased focus with respect to overall functionality, performance and safety. The strong operational requirements have also resulted in increased focus on the total vessel concept and the interactions between the different equipment and systems installed. Flexibility in operation has enabled electrical drives and power generation and distribution systems for propulsion and positioning, where all power and automation equipment are integrated into a

common power plant network and automation network. Positioning systems have been commercially available since the 1960s. However, it was not until the 1990s that fully integrated electrical power, automation and positioning systems became commercially available.

The positioning systems include different control functions for automatic positioning and guidance, see Fossen (1994), Sørensen et al. (1996) and Strand et al. (1997) and the references therein. The positioning controller computes commanded forces in surge and sway, and moment in yaw. The thrust allocation algorithm determines the corresponding force and direction each thruster and propeller device must produce in order to fulfil the positioning controller commands (Fig. 1). By using advanced mathematics based on singular value decomposition and geometrical filtering techniques (Sørdalen, 1996 and 1997), optimal force and direction for each thrust device can be found avoiding singular thrust behaviour with reduced wear and tear and energy consumption for any thrust configuration and type of thruster.

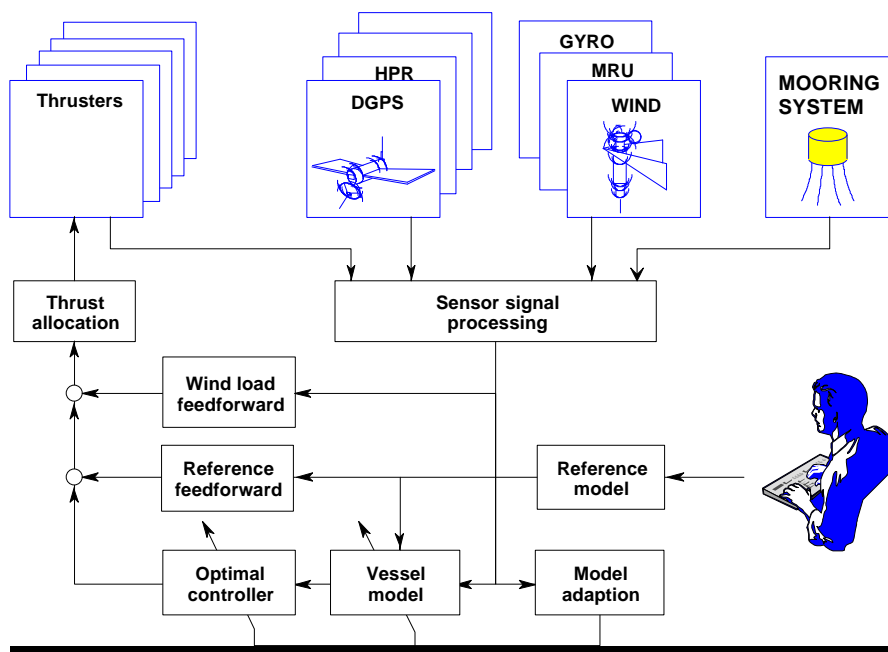


Fig. 1. The positioning controller structure.

Conventionally, the final thruster pitch or speed set-point signals are determined from stationary propeller force to speed/pitch mappings based on information about thruster characteristics and bollard pull tests provided by the thruster manufacturer. These relations may later be modified during sea trials. However, they are strongly influenced by the local water flow around the propeller blades, hull design, operational philosophy, vessel motion, waves and water current. Defectiveness in these nominal mappings from the actual situation due to local water flow phenomena are not directly compensated for in the control system, resulting in reduced positioning performance with respect to accuracy and response time. In addition, deterioration of performance and stability in the electrical power plant network due

to unintentional peaks or power drops caused by load fluctuations on the propeller shafts will occur. The unpredictable load variations force the operator to have more available power than necessary in order to prevent black out situations. This implies that the diesel generators will get more running hours at lower loads in average, which in terms gives more tear, wear and maintenance. A total integrated electrical power, automation and positioning system with functional integration will make the method of thrust allocation based on a combination of torque and power control of the propeller and thruster devices into an attractive and feasible solution to solve these problems.

### **TOTAL INTEGRATED SOLUTION**

The safety and automation system required to monitor and control the power plant, propulsion and thruster system, and the process plant, becomes of increasing importance for a reliable and optimum use of the installation. Cost-saving and fast pay-pack on investments have lead to shorter lead times for electrical equipment, typically less than one year from order to installation. The engineering effort in early design stage has been reduced compared to traditional offshore projects, leaving more engineering to be accomplished in parallel with detailed design, construction, and manufacturing. This new reality defines challenges for owners, yards, and suppliers with little place for the classical offshore engineering processes, which are time consuming and expensive, and more responsibility for the yard to design and interface systems. Since many yards and operators are not structured to accomplish this work, more of this responsibility has been transferred to the suppliers. The trend in the market is towards larger system responsibility for vendors of larger packages. In the market of marine power, automation and positioning systems, there is a handful of vendors more or less able to offer total integrated solutions as shown in Fig. 2. The change in methods and design philosophy is driven by mutual interest of the actors in the market for the following main reasons:

- One contractual partner.
- Reduced risk for customer during construction, commissioning and operation by single system responsibility avoiding sub-optimisation, mismatch and divergence in interfacing and functionality.
- Simplified engineering and installation, since functionality and interfaces are built in well proven product standards.
- Single point of process signal interface and use of fieldbus process I/O give reduced cabling, installation and commissioning costs.
- Reduced maintenance and extent of spare parts in the unified system.
- Higher system integrity.
- Safe and ergonomic operation based on uniform man-machine philosophy for all systems.
- Better overall performance and stability by utilising the potential of functional integration.
- Uniform training and documentation.
- Financing.

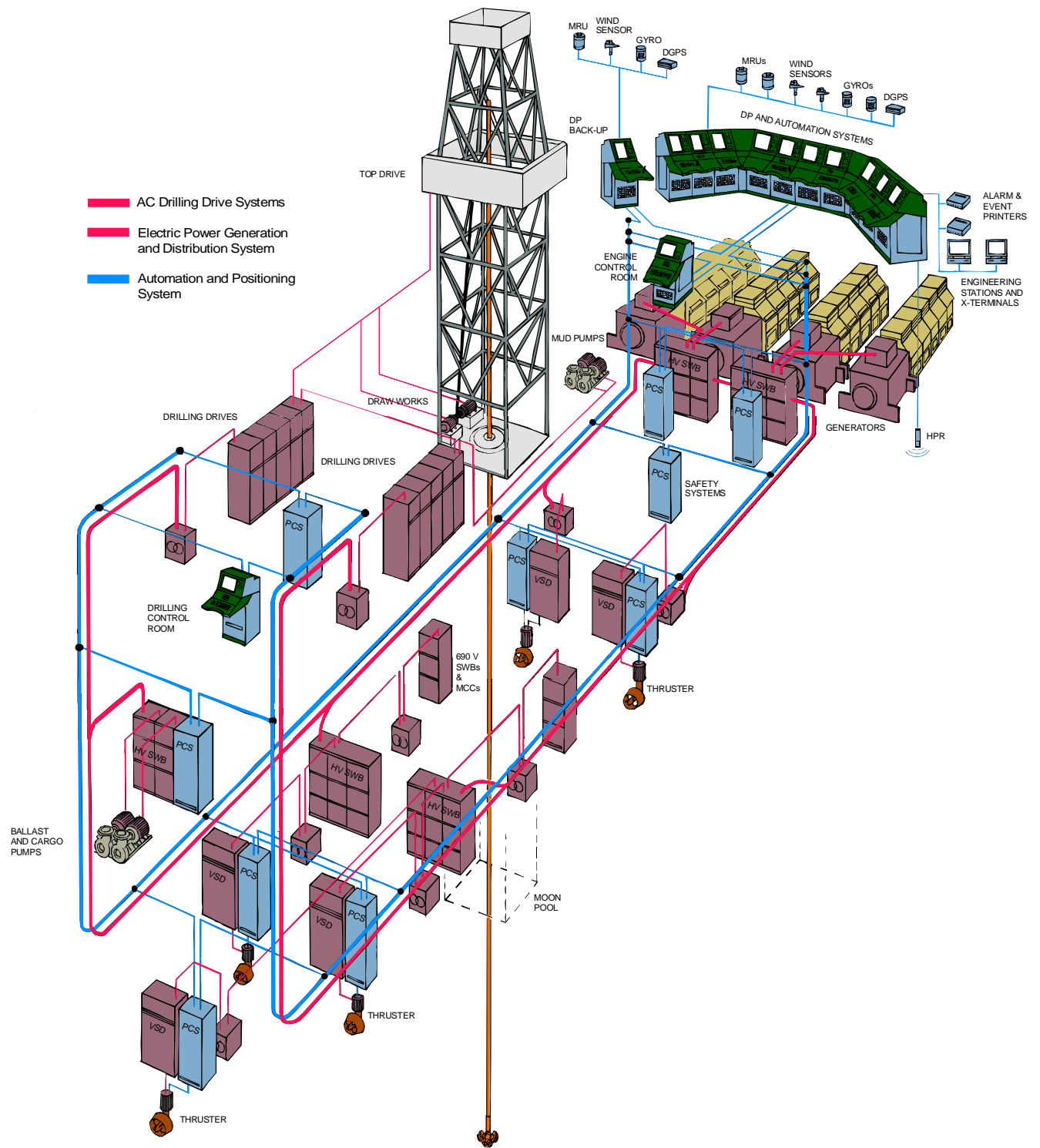


Fig. 2 Drill ship with total integrated power, automation and positioning system.

## MATHEMATICAL MODELLING

### Propeller Characteristics

The propeller thrust  $F$  and torque  $T$  are formulated according to:

$$\underline{F = \rho D^4 K_T |n|n}, \quad (1)$$

$$\underline{T = \rho D^5 K_Q |n|n}, \quad (2)$$

where  $\rho$  is the water density,  $D$  is the propeller diameter, and  $n$  is the propeller speed (revolutions per second). The expressions for  $K_T$  and  $K_Q$  are found by so-called *open water* tests, usually performed in a cavitation tunnel or a towing tank.  $J$  is the advance ratio defined as:

$$\underline{J = \frac{V_a}{nD}}, \quad (3)$$

where  $V_a$  is the inflow water velocity to the propeller. The open water propeller efficiency in undisturbed water is given as the ratio of the work done by the propeller in producing a thrust force divided by the work required to overcome the shaft torque according to:

$$\underline{\eta_o = \frac{V_a F}{2\pi n T} = \frac{J}{2\pi} \cdot \frac{K_T}{K_Q}}. \quad (4)$$

$K_T$ ,  $K_Q$ , and  $\eta_o$  curves for different pitch ratios  $P/D$  for a Wageningen B-screw series based on Table 5 in Oosterveld and van Oossanen (1975), with Reynolds number  $R_n = 2 \times 10^6$ , number of propeller blades  $Z = 4$ ,  $D = 3.1$  m and expanded-area ratio  $\underline{A_E / A_o} = 0.52$  are shown in Fig. 3.

### Propulsion Efficiency

The difference between the ship speed  $U$  and  $V_a$  over the propeller disc is called the wake. For a ship moving forward,  $V_a$  is less than  $U$  since the afterbody flow changes its magnitude between ship speed near the vessel and zero far from the vessel. This *stationary* relationship for axial water inflow can be modelled as (Walderhaug, 1992):

$$\underline{V_a = U(1 - w)}, \quad (5)$$

where  $w$  is the wake fraction number, typically in the range of  $0 < w < 0.4$ . The suction of the propeller generally reduces the pressure at the stern resulting in increased drag, such that the effective thrust becomes:

$$\underline{F_e = F \cdot (1 - t_d)}, \tag{6}$$

where  $t_d$  is the thrust-deduction coefficient, typically in the range of  $0 < t_d < 0.2$  caused by pressure reduction due to potential effects, viscous effects, waves, and appendices (Walderhaug, 1992). In some extreme cases  $t_d$  may become negative. The thrust coefficient behind the hull is normally assumed to be unchanged compared to open water, while the torque coefficient will be affected by the change in inflow at the stern. This is accounted for by the relative rotative efficiency:

$$\underline{\eta_r = \frac{\eta_B}{\eta_o} = \frac{\frac{J}{2\pi} \frac{K_T}{K_{QB}}}{\eta_o} = \frac{K_Q}{K_{QB}}}. \tag{7}$$

The overall propulsion efficiency can now be found as the ratio between the useful work done by the product of effective thrust and ship speed divided by the work required to overcome the shaft torque:

$$\underline{\eta_p = \frac{F_e U}{2\pi n T} = \eta_h \eta_o \eta_r \eta_m}. \tag{8}$$

where  $\underline{\eta_h = \frac{1 - t_d}{1 - w}}$  is defined as the hull efficiency and is according to Newman (1977) in the range of 1.0-1.2.  $\eta_m$  is the mechanical efficiency typically in the range of 0.8-0.9.

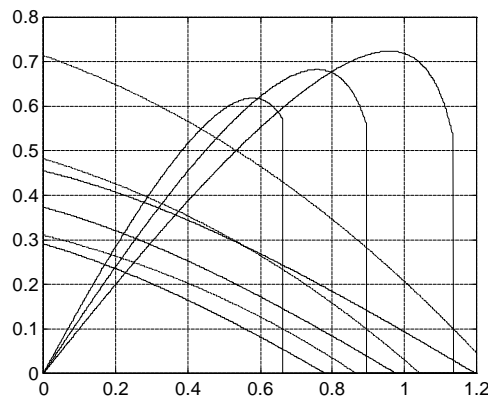


Fig. 3 Open water  $K_T$  (solid),  $10 \cdot K_Q$  (dash-dot) and  $\eta_o$  (solid) as a function of advance ratio  $J$  for  $P/D=0.7, 0.89$  and  $1.1$ .

## Propeller Losses

In addition to the modelled propeller losses caused by axial water inflow, several other effects will contribute to reduction of propeller thrust and torque (Lehn, 1992), such as:

- Water inflow perpendicular to the propeller axis caused by current, vessel speed or jets from other thrusters will introduce a force in the direction of the inflow due to deflection of the propeller race. This is often referred to as cross-coupling drag.
- For heavy loaded propellers ventilation (air suction) caused by decreasing pressure on the propeller blades may occur, especially when the submergence of the propeller becomes small due to vessel's frequency wave motion.
- For extreme conditions with large vessel motions the in-and-out-of-water effects will result in sudden drop of thrust and torque following a hysteresis pattern.
- Both thrust reduction and change of thrust direction may occur due to thruster-hull interaction caused by pressure effects when the thruster race sweeps along the hull. This is referred to as the Coanda effect.
- Thruster-thruster interaction caused by influence from the propeller race from one thruster on neighbouring thrusters may lead to significant thrust reduction, unless appropriate precautions are taken in the thruster allocation algorithm.

The sensitivity to the different types of losses depends on which type of propeller and thruster used, application of skegs and fins, hull design and operational philosophy (Lehn, 1992). Main propellers are subject to large thrust losses due to air ventilation and in-and-out-of-water effects. Rotatable azimuth thrusters are subject to dominating losses caused by hull friction and interaction with other thrusters. Tunnel thrusters are subject to losses caused by non-axial inflow due to current and vessel speed and ventilation phenomena in heavy weather.

## Propeller Shaft Model

The torque balance for the propeller shaft is shown in Fig. 4, where  $T_m$  is the torque generated by the thruster motor,  $J$  is the moment of inertia for the shaft, and  $\omega = 2\pi n$  is the angular shaft speed. The power delivered by the motor is given by:

$$\underline{P_m = \omega T_m = 2\pi n T_m}, \quad (9)$$

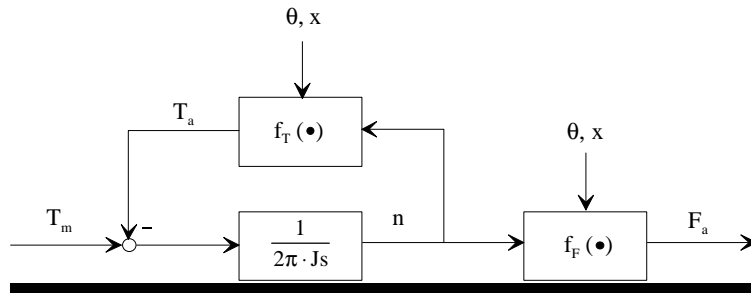


Fig. 4 Propeller shaft model (*s* denotes the differential operator).

### Torque Loop in an Electrical Motor Drive

The torque control is inherent in the design of most applied control schemes for variable speed drive systems. The torque is controlled by means of motor currents and motor fluxes with high accuracy and bandwidth, see Fig. 5. Theoretically the rise time of the torque in PWM (Pulse Width Modulated) drives is limited by the motor's inductance (in load commutated inverters, LCI's, also by the DC choke). However, in practice the controller limits the rate of change of torque in order to prevent damages on the mechanics. The torque controller may for practical reasons be assumed to be equivalent to:

$$T_m(s) = \frac{1}{1 + T_T s} T_c(s) \tag{10}$$

where the time constant  $T_T$  is in the range of 20-200 ms.

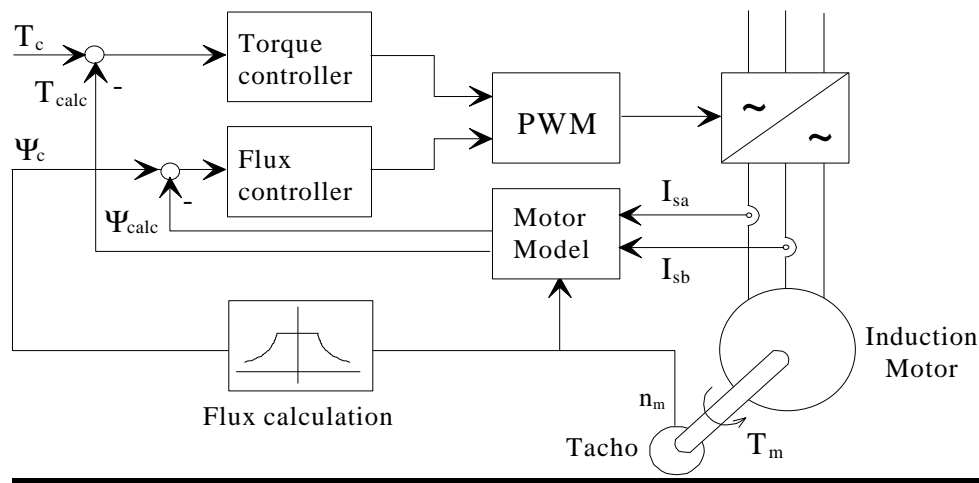


Fig. 5 Torque loop in electrical motor drive.

## CONTROLLER DESIGN

### Speed Control

In conventional FPP systems a speed controller is used to achieve the commanded propeller force, as shown in Fig. 6. The reference (commanded) speed in the propeller  $n_{ref}$  is found by the stationary function:

$$n_{ref} = g_{n0}(F_{ref}) = \text{sgn}(F_{ref}) \sqrt{\frac{F_{ref}}{\rho D^4 K_{T0}}}, \quad (11)$$

which is the inverse function of the nominal shaft speed-versus-force characteristics given in (1) for typically  $K_{T0} = K_T(J = 0)$ .

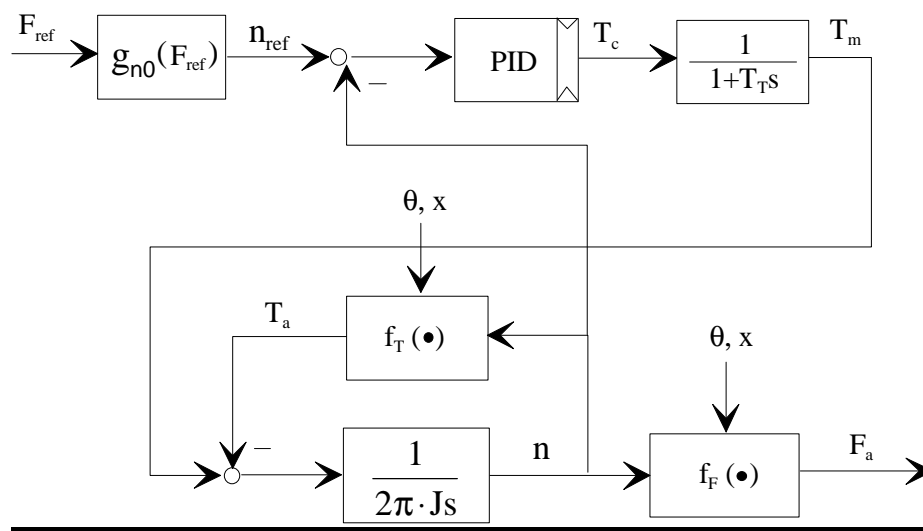


Fig. 6 Speed controlled propeller.

The rated (nominal) torque and power are denoted  $T_N$  and  $P_N$ . The speed controller is a PID controller with saturation limits, which calculates the necessary torque to obtain increased/decreased speed. The maximum torque is typically in the range of 1.1 - 1.2 higher than the rated torque.

### Torque Control

In the proposed torque control strategy the outer speed control loop is removed, and the thruster is controlled by its torque control loop with a commanded torque  $T_c$  as set-point, Fig. 7. The stationary mapping between the commanded thrust force and the torque can be found to be:

$$\underline{T_{ref}} = \frac{DK_{Q0}}{K_{T0}} F_{ref} = g_{T0}(F_{ref}) \tag{12}$$

where typically  $K_{Q0} = K_Q(J=0)$ . To the existing torque loop a new function, *Torque algorithm*, is added (Fig. 8).  $F_{ref}$  is the commanded propeller force as before. The torque reference is filtered through a reference generator, which yields smooth desired torque references  $T_d$  and  $\dot{T}_d$ .

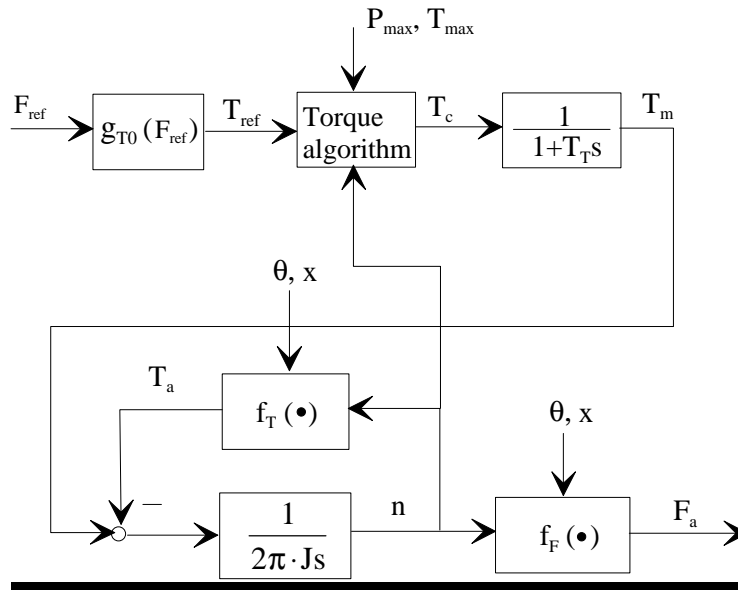


Fig. 7 Torque controlled propeller.

In order to speed up the response a reference feedforward control action is computed. The commanded torque must also be limited by the maximum torque capability  $T_{max}$  and power capability  $P_{max}$ .

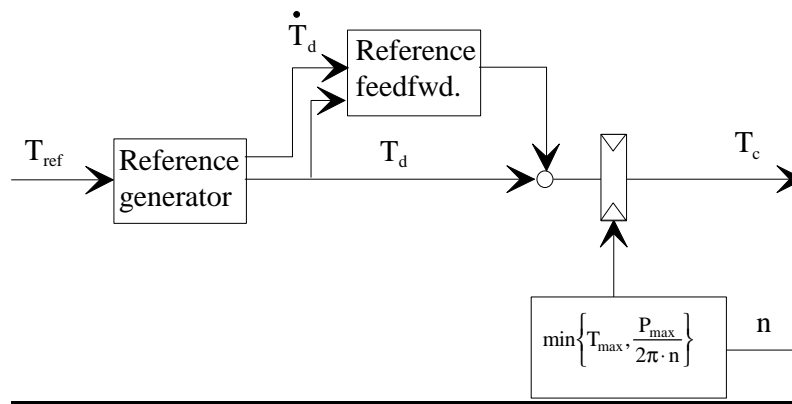


Fig. 8 Commanded torque algorithm.

The torque limiting function is described in Fig. 9. The torque must also be limited by the maximum power, which yields hyperbolic limit curves for the torque as a function of speed. Since maximum power is not limited by the converter and motor ratings only, but also by the available power in the generators, this limit will vary accordingly. By this method the power limitation will become fast and accurate, allowing to utilise the power system's power capability with a built-in black out prevention.

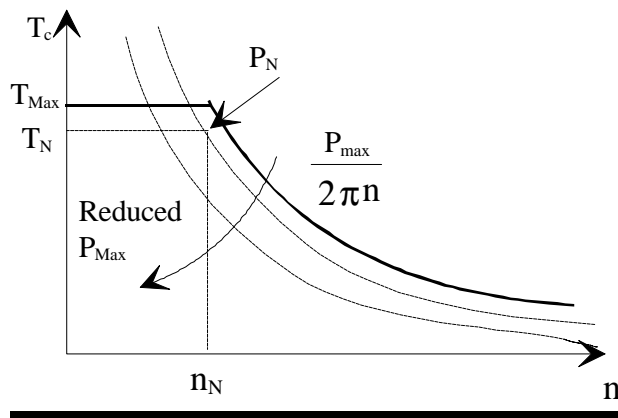


Fig. 9 Torque limitation.

**Power Control**

An alternative control strategy for propeller control based on power control is also investigated. The torque control loop is maintained, but the commanded torque is found from a commanded power  $P_{ref}$  (Fig. 10). This power reference is a signed value in order to determine the torque direction. The mapping between the reference thrust force and the power can be written:

$$P_{ref} = \text{sgn}(F_{ref}) \frac{2\pi K_{Q0}}{\sqrt{\rho D K_{T0}^{3/2}}} |F_{ref}|^{3/2} = g_P(F_{ref}). \tag{13}$$

As for the torque loop a new function, *Power algorithm*, is added.

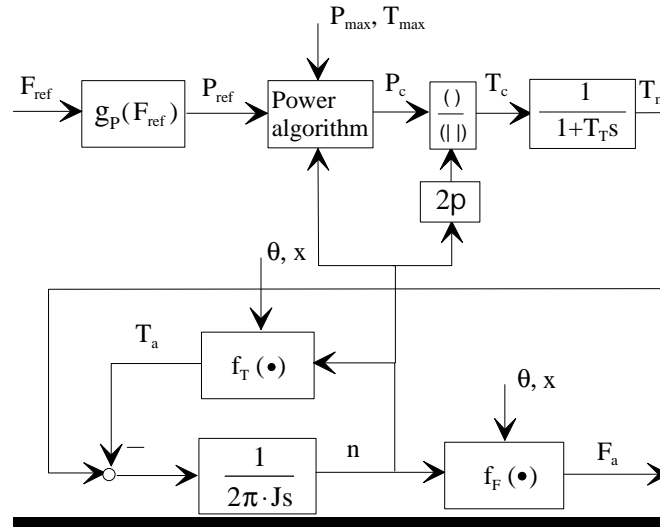


Fig. 10 Power controlled propeller.

The power reference is filtered through a reference generator, which yields smooth desired torque references  $P_d$  and  $\dot{P}_d$ . In order to speed up the response a reference feedforward control action is computed.

**Sensitivity to Thrust Losses**

In order to compare the different control schemes a simplified sensitivity analysis was carried out in Sørensen et al. (1997) to address the most significant properties of speed control, torque control and power control. Pitch control was not studied, but is expected in general to have the same behaviour as speed control.

Fig. 11 clearly shows the performance for the different control schemes by means of sensitivity functions (actual thrust relatively to desired thrust), for  $t_d = 0$ ,  $h_F = h_T = 1$  and  $K_{T0} = K_T(J = 0)$  and  $K_{Q0} = K_Q(J = 0)$  with the same parameters as used in Fig. 3. for  $P/D = 0.98$  as a function of advance ratio  $J$ , see Fig. 11. As expected, all three sensitivity functions decrease, resulting in increased thrust losses, for increasing  $J$ . The speed control scheme is less robust for variations in  $J$ , while the torque control scheme shows the best robustness.

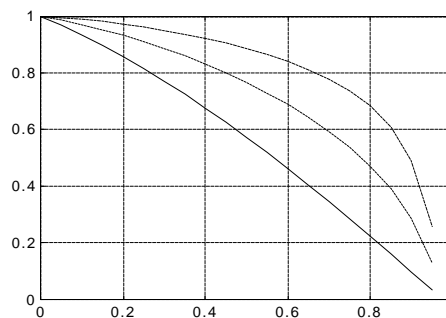


*Fig. 11 Sensitivity functions for the different control schemes: speed control  $s_n$  (solid), power control  $s_p$  (dash), and torque control  $s_T$  (dash-dot) as function of advance ratio  $J$  for  $P/D = 0.89$ .*

### Electrical Power Plant Network Performance and Stability

The power plant on ships consists of several gas turbine or diesel engines driving electrical generators. For safe operation there must in all load conditions be enough spinning reserves with sufficient available power for unpredicted variations in load in order to prevent black-out. The black-out prevention by means of reducing load on heavy consumers must typically respond faster than 500 ms to be effective. With torque and power control, the propeller load is less sensitive to variations in the surroundings, giving less power disturbances on the network and improved voltage and frequency quality. Additionally, the maximum power consumption may easily be limited to the available power in both schemes, since the power limitation is explicit in the torque and power control algorithm. This in contrast to speed controlled and pitch controlled propellers, where the actual power load must be measured as a feedback signal with an inherent time lag which deteriorates the black-out prevention response time. The accurate and fast control of power and power limitation in torque and speed control gives less unpredicted load changes, and less need for available power. The number of running generators can be reduced, and the average loading will be higher. This in terms gives less tear, wear, and maintenance of the prime movers.

### SIMULATIONS

Numerical simulations are carried out in order to illustrate the properties of the different control schemes with respect to the positioning performance and the corresponding effects on the electrical power plant network. As for the example above only thrust losses due to axial water inflow according to (5) are considered. It is assumed that the propeller has  $P/D = 0.89$ . The propeller is exposed to axial current equal to 1 m/s and waves described by a Pierson-Moskowitz spectrum with significant wave height  $H_s = 3.0$  m,  $T_p = 10$  s. A constant propeller force reference (set-point)  $F_{ref} = 100$  kN is commanded. In Fig. 12a the effect on propeller speed (RPM) is shown. For the speed control scheme the corresponding speed set-point is equal to 100.9 RPM. As expected the power and torque control schemes will produce higher speed in order to compensate for the losses experienced. In Fig. 12b the effect on motor torque is shown. For the torque control scheme the corresponding torque set-point is equal to 40.0 kNm. As expected the power and torque control schemes will produce higher torque in order to compensate for the losses experienced.

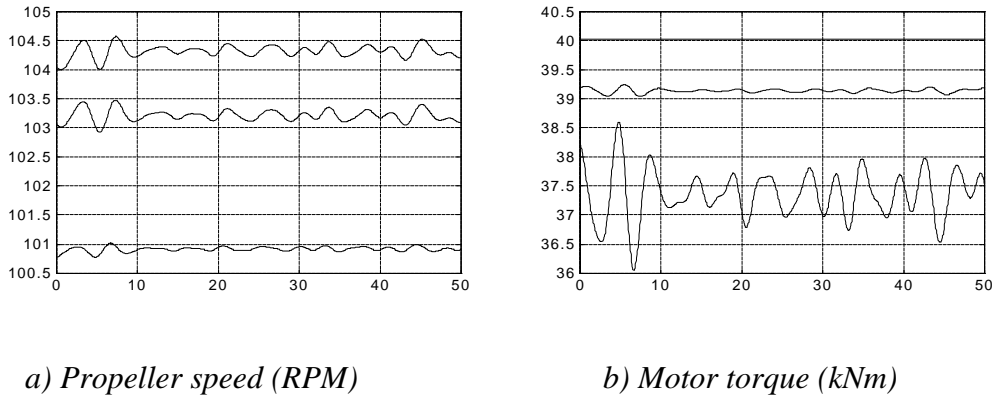


*Fig. 12 Propeller speed and motor torque applying speed control (lowest), power control (middle) and torque control (upper).*

In Fig. 13a the effect on motor power is shown. For the power control scheme the corresponding power set-point is equal to 423 kW. It is clearly seen that the power control scheme results in lowest power peaks, while the speed control results in highest power variance. In Fig. 13b the actual propeller force produced is shown applying the speed control scheme (lowest), the power control scheme (middle) set and torque control (upper). The stationary offset in actual produced propeller force compared to the propeller force reference (set-point)  $F_{ref} = 100$  kN can after a period of time be compensated by the feedback action in the positioning controller. However, the time lag for such a compensation results in reduced positioning performance (bandwidth).

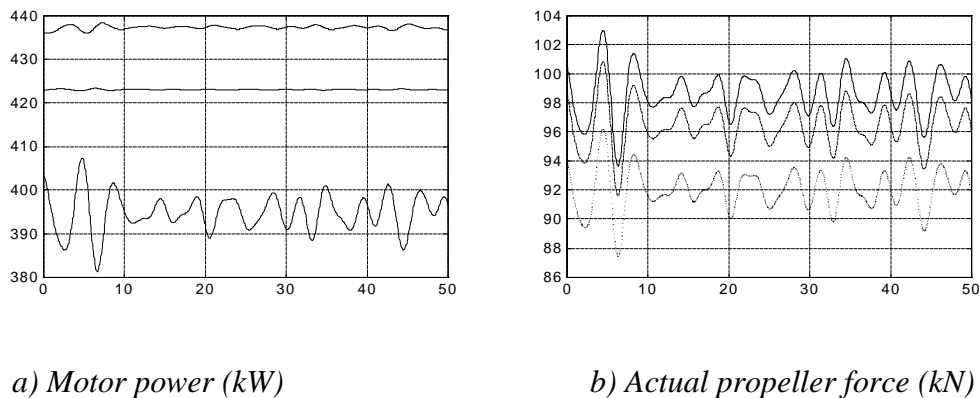


*Fig. 13 Motor power and actual propeller force for speed control (lowest), power control (middle) and torque control (upper).*

**CONCLUSIONS**

A new method based on moment and power control of the propeller and thruster devices is proposed by utilising the potential of functional integration of the fully integrated electrical power, automation and positioning system. Instead of calculating the speed and pitch set-point

based on a force to speed/pitch relation, force to moment and force to power relations are used. This method gives a significant improvement in the performance of the positioning accuracy due to improved robustness with respect to thrust losses. In addition the performance and the stability of the electrical power plant network are improved due to more direct access and control of the actual power consumption from the thruster system. Simulations illustrate the difference in performance and power plant stability of the different control schemes. Torque control has been shown to have the lowest sensitivity in obtained thrust with respect to disturbances and thrust losses, and is thus the most robust control strategy among the evaluated alternatives. The variance in power is some higher than for power control, giving more disturbances in the power network. Where power variation and quality are essential, the power control may be an alternative. However, the performance at low speeds and thrust demand is expected to be poor, since small variations in power reference gives large variations in thrust. Hence, the algorithm will be highly sensitive to modelling errors. For such applications, a combination of these two strategies, where torque control is dominating at low speed and power control at higher speed will be applied.

*ACKNOWLEDGEMENTS* - ABB Industri AS, Marintek AS and The Research Council of Norway are gratefully acknowledged for fruitful co-operation and contributions.

## REFERENCES

- Fossen, T. I. (1994). *Guidance and Control of Ocean Vehicles*. John Wiley and Sons Ltd.
- Lehn, E. (1992). *Practical Methods for Estimation of Thrust Losses*. Marintek Report MT51A92-003, 513003.00.06.
- Newman, J. N. (1977). *Marine Hydrodynamics*. MIT Press, Cambridge, Massachusetts.
- Oosterveld, M. W. C. and P. van Oossanen (1975). Further computer-analyzed Data of the Wageningen B-screw Series. *Int. Shipbuilding Progress*, Vol. (22), pp. 251-262.
- Strand, J.-P., A. J. Sørensen and T. I. Fossen (1997). Modelling and Control of Thruster Assisted Position Mooring Systems for Ships. 4th IFAC Conference on Manoeuvring and Control of Marine Craft (MCMC'97), Brijuni, Croatia, pp. 160-165.
- Sjørdalen, O. J. (1996). Thruster Allocation: Singularities and Filtering. IFAC World Congress, SF, CA, Vol. (Q), pp. 369-374.
- Sjørdalen, O. J. (1997). Optimal Thrust Allocation for Marine Vessels. *IFAC J. of Control Engineering Practice*, Vol. (5), No. 9, pp. 1223-1231.
- Sørensen, A. J., S. I. Sagatun and T. I. Fossen (1996). Design of a Dynamic Positioning System Using Model-Based Control. *IFAC J. of Control Engineering Practice*, Vol. (4), No. 3, pp. 359-368.

Sørensen, A. J., A. K. Ådnanes, T. I. Fossen and J.-P. Strand (1997). A New Method of Thruster Control in Positioning of Ships Based on Power Control. 4th IFAC Conference on Manoeuvring and Control of Marine Craft (MCMC'97), Brijuni, Croatia, pp. 172-179.

Walderhaug, H. (1992). *Motstand, Framdrift, Styring*. Lecture Notes, Department of Marine Hydrodynamics, Norwegian University of Science and Technology (in Norwegian).